Engineered Science
DOI: https://dx.doi.org/10.30919/es903

Electrochemical Detection of Uropathogenic Escherichia coli Using Polyvinylalcohol/r-Graphene Oxide/Polyethylenimine Modified Nanocomposite Electrode

P. Parthasarathy

Abstract

Detecting microorganisms quickly and selectively is extremely important in clinical analysis and in monitoring the quality of food and water. This study details the development of a biosensor that uses electrochemical methods to selectively detect uropathogenic Escherichia coli (E. coli) bacteria in both aqueous and serum samples. The biosensor is developed using a simple and cost-effective method involving reduced graphene oxide (r-GO) with PVA (Polyvinylalcohol) and PEI (Polyethylenimine) through a Sol-Gel spin coating process. The numerous NH_2 groups on the PVA and PEI are used to functionalize the biosensor's surface. To increase the specificity of the detection process, amide bonds are formed on the electrode surface using anti-fimbrial E. coli antibodies. The redox mediator prevents the formation of immunological complex and it enhances the transmission of electrons from the developed PVA/rGO/PEI-modified layer to detect E. coli. The development of an electrochemical test for E. coli illustrates the efficacy of these biosensors. Using only 5 µL of sample, it is discovered that these biosensors have a broad dynamic range (915-2.5×10^7 CFU/mL) and low limits of detection (285 CFU/mL). Moreover, the biosensor performs well in aqueous, serum, and urine media, making it potentially useful for the clinical diagnosis of pathogenic diseases. This study highlights the potential of these biosensors for real-world, point-of-care applications.

Keywords: Polyvinylalcohol, Reduced graphene oxide, Polyethylenimine, Escherichia coli, Electrochemical Detection, Nanocomposite Synthesis.
Received: 21 March 2023; Revised: 26 April 2023; Accepted: 29 May 2023.
Article type: Research article.

1. Introduction

The most common bacterial infectious disease in humans is urinary tract infection (UTI), and Escherichia coli (E. coli) is the most frequent pathogen, causing 30-50% of UTIs acquired in hospitals and 80-90% of UTIs obtained in the community. It is vital to identify distinct bacterial strains and recognise pathogenic E. coli at extraordinarily low concentrations because they emit virulence factors that may cause illness in the host tissues. Culture-based methods used in conventional methods for identifying and detecting bacteria are labour-intensive, complicated, and inappropriate for on-site monitoring.[1] They also require a microbiology laboratory and are labour-intensive. Hence, there is a critical need for quick, efficient, selective, and highly sensitive bacterial detection, and biosensors are essential in achieving these goals. Graphene-based sensors, particularly graphene-based field effect transistors, enable pathogen detection (GFETs). The promise of biosensors for real-world applications has been shown in a number of studies using anti-E. coli antibody-modified CVD graphene or thermally-reduced graphene oxide sheets (rGO) for the sensitive and selective detection of E. coli with low limits of detection.[2-4] Under ideal conditions, Chen et al. were able to detect E. coli O157:H7 with a detection limit of 803 CFU mL^{-1} using holey rGO functionalized with Magainin I as the transducer element in a GFET. For the quick and precise detection of infections, an affordable, easy-to-use, and portable electrochemical detection approach by impedimetric methods is very alluring. In addition, voltammetric and amperometric immunoassays are often used as label-free methods for detecting pathogens. Ahmed et al. developed an antibody-based immunological sensor with a linear response of 102-105 cells to identify S. pyogenes in human saliva. Graphene nanostructures have been used in electrochemical sensors to increase their sensitivity.[5] Recent

CMR Institute of Technology, Bengaluru - 560037, Karnataka, India.
**Email:* arjunsarathii@gmail.com (P. Parthasarathy)

work has focused on creating electrochemical immunosensors for the detection of dangerous microbes using graphene composite electrodes (a schematic of the same is depicted in Fig. 1). The illustration below[6] shows how bio-functionalized rGO nanocomposite electrochemical biosensors are used to find foodborne harmful microorganisms. Panel A shows the various kinds of biomolecules that have been converted into rGO nanocomposites, whereas Panel B presents several electrochemical biosensors that have been employed to detect foodborne harmful bacteria.[7,8]

In comparison to other sensing methods, electrochemical biosensors provide a number of benefits, such as low cost, high sensitivity, and quantitative output. Due to its high surface area, variety of functions, and biocompatibility, graphene-based electrodes hold considerable potential for the development of sensitive electrochemical sensors for applications in healthcare, food safety, and environmental monitoring. However, there are drawbacks to the conventional approaches for manufacturing low-defect graphene by physical exfoliation or chemical vapour deposition (CVD), such as the need for costly or hazardous solvents and time-consuming transfer operations.[9-11] A potential solution to these problems in the fabrication of graphene electrodes is to use functionalized graphene, such as graphene oxide (GO). Nevertheless, GO cannot be employed in electrical equipment due to its low electrical conductivity. Reduced graphene oxide (rGO), which has a high electron transfer rate, strong electrical conductivity, and enough oxygen groups for future functionalization, provides a solution to this problem. Chemical, thermal, and electrochemical processes for converting GO to rGO have all been investigated. These methods have been used to produce graphene electrodes with various surface compositions and defect concentrations.[12] Making laser-induced graphene (LIG) electrodes is one way to pattern graphene. This method allows for the simultaneous reduction and patterning of GO or the production of graphene and is simple, effective, inexpensive, chemical-free, and mask-free. The Kaner group has already produced LIG electrodes for under $20 using the LightScribe DVD driver. Although polyimide substrates are frequently utilized in the industry, research has also been done on substitute materials such as other polymers, carbon, and natural materials.[12,13] Nevertheless, there is no evidence that biosensors have been produced using electrodes made by laser-induced reduction of GO. Instead, there have been papers on the production of electrodes and the development of biosensors using electrodes made by laser-scribing polyimide sheets. The in-situ reduction method places GO and rGO in the same plane, which poses two significant difficulties for the creation of this kind of biosensor. Moreover, LIG is easily fractured and brittle. A method for transferring LIG from polyethene terephthalate was developed by the Nam group, however, it can only be used on substrates that don't absorb the excitation laser.[13,14]

In this paper, we described the production of reduced graphene oxide electrodes in an effort to simplify and scale up the process. We also demonstrate improved graphene oxide biosensing abilities using polyvinyl Alcohol (PVA) and polyethylenimine (PEI).[15] The created sol-gel nanocomposite was spin-coated with ITO coatings onto glass substrates. A nanocomposite electrode-based biosensor that has been created as a proof-of-concept can be utilized to identify E. coli using an electrochemical ELISA and Chronoamperometry. The sensor was examined using a portable commercial Potentiostat and tested in both phosphate-buffered saline (PBS) and artificial urine (AU), demonstrating its potential for point-of-care applications.

2. Experimental

2.1 Materials

The 10 mg/mL concentration GO water dispersion was bought from Sigma Aldrich. Kesari Scientific Chemicals provided tryptic soy agar, Tween 20, and phosphate-buffered saline tablets. To create a buffer solution with a pH of 7.4 and a concentration of 10 mM, PBS tablets were dissolved in ultrapure water. Moreover, a (phosphate-buffered saline with Tween 20) PBST buffer solution containing 10 mM PBS and 0.05 wt% Tween 20 was created.[16–18] Sigma Aldrich provided the polyclonal anti-E. coli antibody (PA1-7213) and Alfa

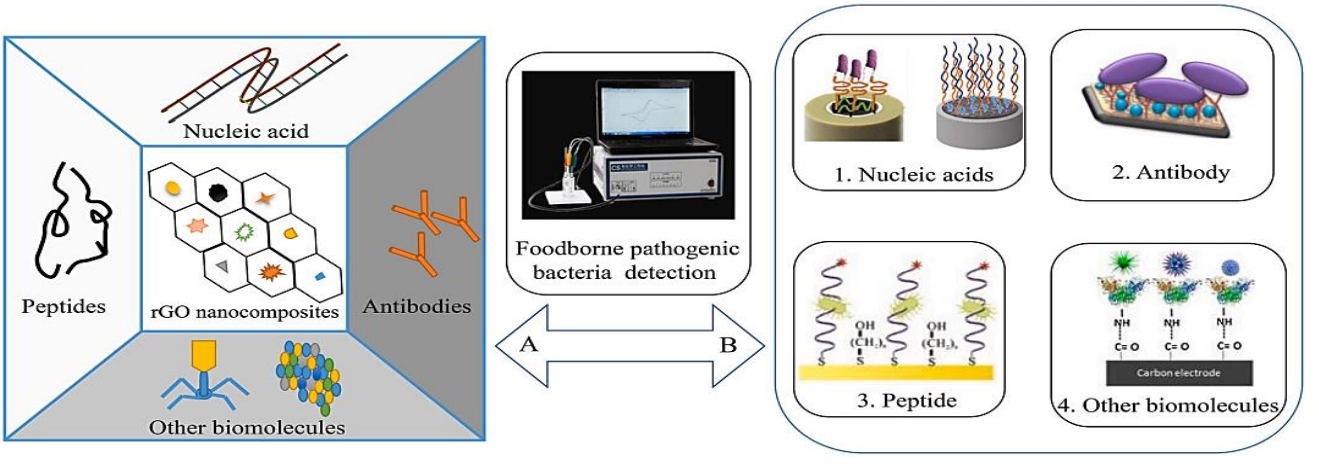

Fig. 1 The figure illustrates the use of bio-functionalized rGO nanocomposite electrochemical biosensors for the detection of foodborne pathogenic bacteria.

Aesar provided the antibodies that were HRP-labelled (ab20425). E. coli was purchased in Bombay from ICT (E. coli, CECT 4972).

2.2 Electrode preparation

In this study, a combination of graphene oxide (1 mg/mL), Polyethylenimine (1 mg/mL), and polyvinyl alcohol (GO/PEI/PVA) was stirred for 32 hours at room temperature to create an aqueous dispersion. Reduced graphene oxide/Polyethylenimine/ovalbumin (rGO/PEI/OVA) was added to the thin film electrode using a spin-coating technique and an aqueous solution. The resulting electrode was used as a working electrode for the electrochemical analysis of E. coli. After being deposited, the electrode surface was washed with Milli-Q water and dried by air.

2.3 Anti-fimbrial E. coli antibody immobilisation on a PVA/rGO/PEG electrode

The electrode was converted into an active electrode by immersing the produced nanocomposite electrode for 4 hours at room temperature in a solution of 1-pyrene butanoic acid succinimidyl ester. The electrode was washed with four rounds of ultrapure water after being turned on, then twice with IPA. The capture antibody (cAb, 15 g/mL in 10 mM PBS) was immobilized by being exposed to 5 µL of the solution on the working electrode (WE) for an overnight duration at 4 °C. For the purpose of stopping any unreacted PBASE, 4 µL of ethylamine, 0.1 M in PBS, was injected into the WE. In order to prevent general fouling under challenging circumstances, the WE was then treated with bovine serum albumin (BSA, 5 L, 5% in PBS) for 1 hour at 37 °C. The electrode was cleaned twice in PBS and twice in PBS with Tween 20 in between each stage (PBST). These procedures were all completed in a humidity chamber. The procedure comprises employing 1-ethyl-3- (3-dimethylaminopropyl) carbodiimide (EDC)/N-hydroxysuccinimide (NHS) crosslinking chemicals to cationically bond anti-fimbrial E. coli antibodies to a PVA/rGO/PEI functionalized gold interface. The NH_2 groups of PEI and the COOH functions of the antibody had chemical interactions. The gold interface was first coated with PVA/rGO/PEI and then agitated for 2 hours at 4 °C in an aqueous solution of the antibody, 1-ethyl-3- (3-dimethylaminopropyl) carbodiimide hydrochloride (EDCHCl), and NHS. PBS was used to rinse the surface to eliminate any remaining antibodies and unreacted components. After that, it was kept at 4°C in a PBS buffer until it was needed.[22]

3. Result and discussion

3.1 Characterization

Cu Kα (λ = 1.54 A) radiation was used with a Bruker D8 Advance X-ray diffractometer to produce the XRD patterns. The findings demonstrated that the typical XRD diffraction peak of pure GO is seen at $2\theta = 10.5^{o}$ in Fig. 2(a, b, and c), indicating a layer separation of approximately 0.84 nm. The

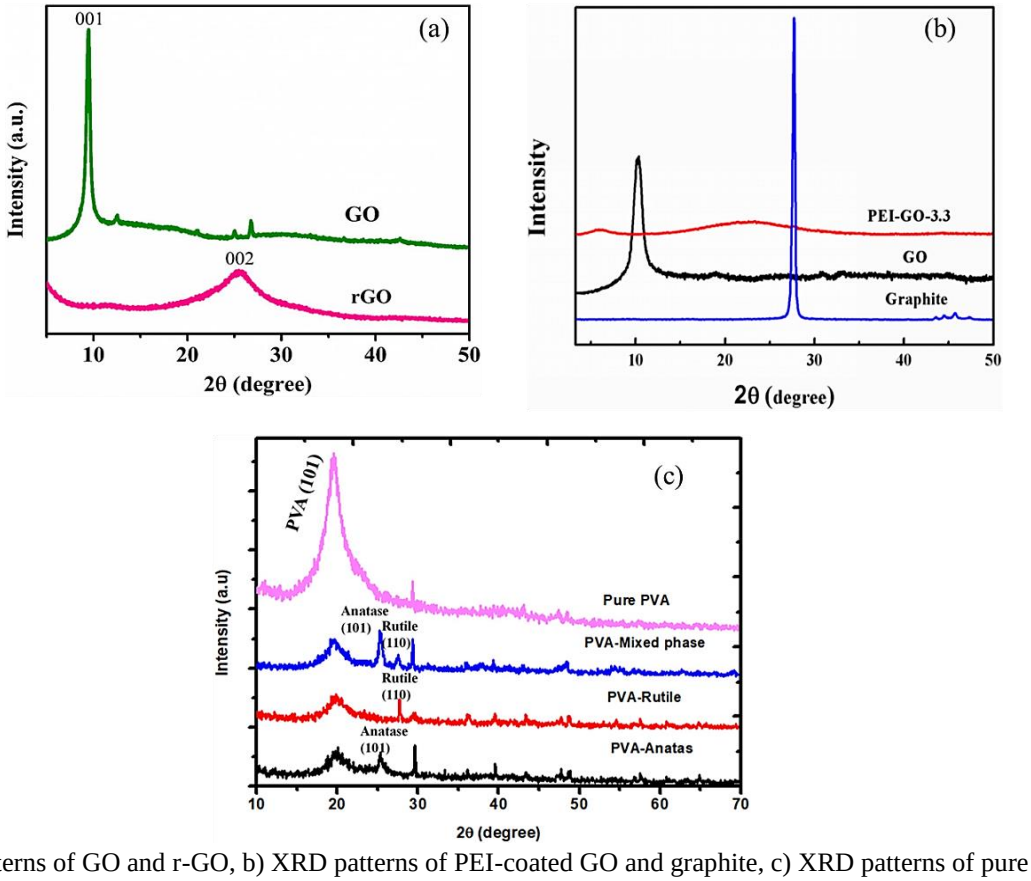

Fig. 2 a) XRD patterns of GO and r-GO, b) XRD patterns of PEI-coated GO and graphite, c) XRD patterns of pure PVA and mixed forms of PVA in three different structures.

XRD diffraction peak for PVA is observed at $2\theta = 20.5^{o}$.[23] It's interesting to note that the rGO/PVA film's XRD pattern only displays one peak at $2\theta = 20.5^{o}$, demonstrating that GO has been evenly distributed throughout the PVA matrix and that rGO could not be restacked during the reduction process. The crystalline structure of PVA was somewhat altered by the insertion of rGO.

The surface's morphology was examined using the thermal field emission emitter-equipped electron microscope ULTRA 55 (Zeiss, France) and a high-efficiency In-lens SE detector (Fig. 3). Using Zeiss Compact Merlin equipment and a high vacuum of 2 kV, pathogen SEM images were captured. The biological samples were coated with a 5 nm-thick ITO-covered glass substrate and treated with a 1% glutaraldehyde solution for 30 min at room temperature in the dark prior to imaging. The photos also showed how optically homogenous the ball-shaped PVA/rGO/PVA films were.

3.2 ELISA bacterial detection

A 50-well ELISA plate was used to conduct the ELISA test. The captured antibody was first applied, and it was then incubated at 5°C overnight. After that, BSA was added to stop nonspecific fouling of the wells, then bacterial samples were added and the wells were incubated for 2 hours at room temperature. Between each stage, PBST was applied three times to the wells. Following the addition of HRP-labelled detection antibodies, the sample was incubated for 2 hours at room temperature before being washed 10 times with PBST. The TMB substrate solution was then added and allowed to sit at room temperature for 20 minutes. A microplate reader was used to measure each well's absorbance at 550 nm after adding 5 M of H_2SO_4 to stop the reaction.

3.3 Electrochemical bacterial detection

Using cyclic voltammetry (CV) and differential pulse voltammetry, the electrochemical characteristics of the developed electrodes were assessed (DPV). The CV and DPV were measured using a cordless portable Potentiostat. An Ag/AgCl reference electrode, a counter electrode, and a working electrode built of a newly developed nanocomposite were used in a typical three-electrode system to test the electrodes (coated over ITO glass slides). Differential pulse voltammetric recordings were made under simulated conditions with a modulation duration of 1 s, an interval time of 1 s, a step potential of 10 mV, and a modulation amplitude of 80 mV. After 35 minutes, the bacteria were discovered after 6 L of the solution containing the bacteria had been pipetted into the working electrode. The electrode was then cleaned four times with PBS and four times with PBST. Pipetting the detection antibody solution (dAb, ab20425, 2 g/mL) onto an electrode and letting it sit for 40 minutes were both successful. After then, the electrode was rinsed five times with PBS and twice with PBST. The chronoamperometric sensing technique was then started after adding the 60 L of TMB ELISA solution. Chronoamperometry (CA) was carried out using the PalmSens4 and an internal wireless Potentiostat developed in accordance with some references[24,25] at +0.225 V against the onboard Ag/AgCl reference electrode.

At varied bacterial concentrations, the PVA/rGO/PEG-anti-fimbrial electrode's sensitivity for detecting E. coli UTI89 was assessed. After the electrode is exposed to E. coli UTI89 for 30 minutes, the $[Fe(CN)_6]_4$ redox probe's DPV peak current is decreased, as shown in Fig. 4a. The variation in current is linearly proportional to the number of UTI89 cells. A calibration curve (Fig. 4b) is generated by monitoring the variability in peak current as a function of pathogen concentration. The linear range of 1100×10^{-1} to 10^4 cfu mL^{-1} and the 96% confidence level indicate that the detection limit for UTI89 is less than 10 cfu mL^{-1}. The technology exhibits its capacity to convert the link between the pathogen and antibody biorecognition into numerical signals. The study examines the dependability and capability of the proposed sensor to identify *E*. coli UTI89 in genuine samples, including human blood and urine spiked with various concentrations of the bacteria. When the electrochemical signals from the experiment are compared to those from PBS, a similar pattern

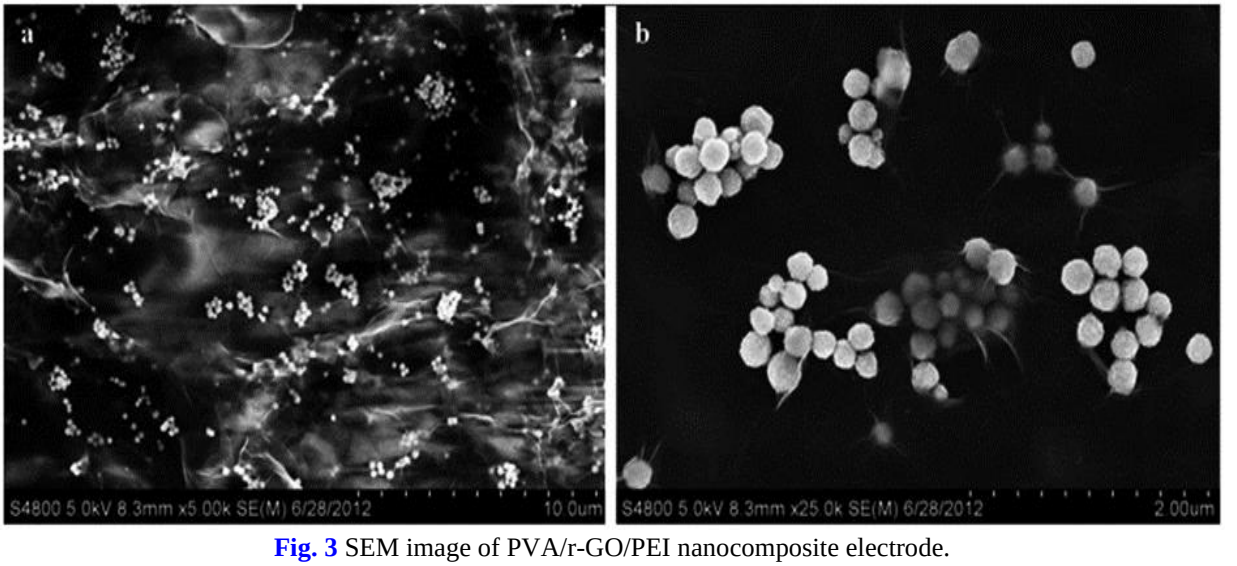

Fig. 3 SEM image of PVA/r-GO/PEI nanocomposite electrode.

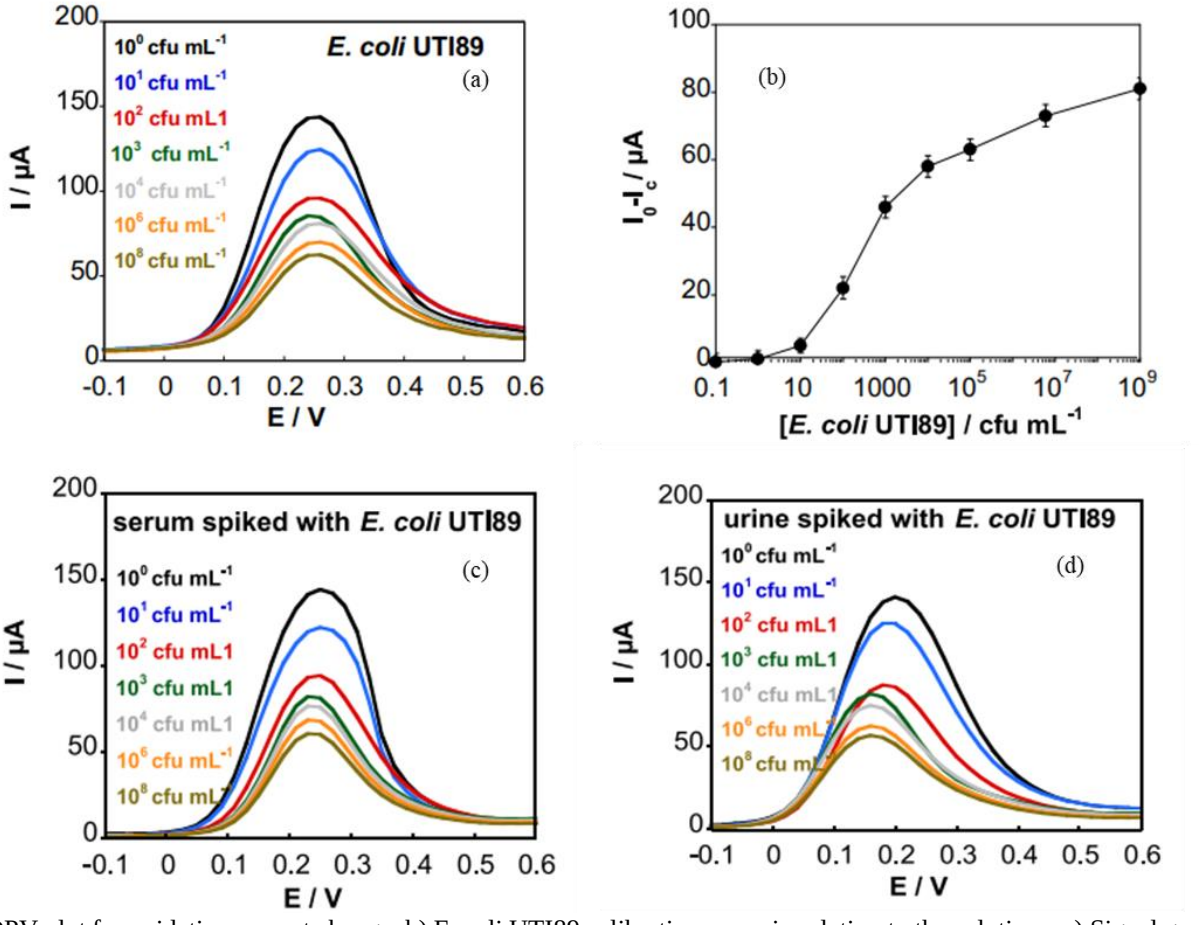

Fig. 4 a) DPV plot for oxidative current change, b) E. coli UTI89 calibration curve in relation to the solutions, c) Signal generated in spiking serum, d) Spiked urine produced at an electrochemical analysis.

of diminishing current with rising bacterial concentration could be seen. The electrochemical signal generated by spiked serum and urine is shown in Figs. 4c and 4d, and Fig. 4b compares the current responses in PBS and spiked human serum and urine. By analysing serum samples contaminated with S. aureus, the sensor's sensitivity for detecting E. coli UTI89 in complicated media was tested.

The lack of any alteration in the electrochemical signal, as shown in Fig. 5, demonstrates the sensor's strong sensitivity to *E*. coli UTI89. The sensor's ability to precisely detect *E*. coli UTI89 in real samples is further tested using human serum samples spiked with both *E*. coli UTI89 and *S*. aureus. The results show that *E*. coli UTI89's observed current response is unaffected by *S*. aureus's absence.

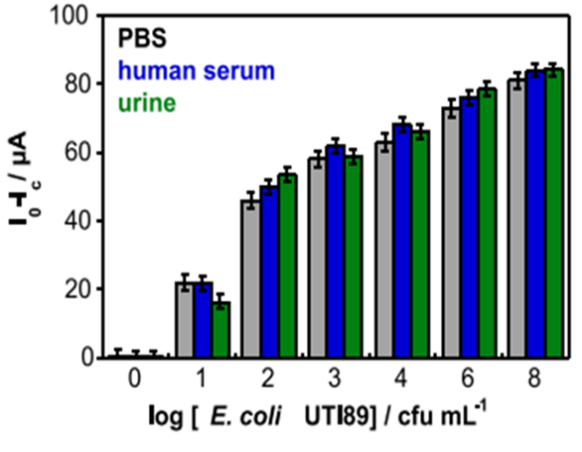

Fig. 5 Anti-fimbrial modified electrode's sensitivity to *E*. coli.

The produced sensors' stability is evaluated under a number of different storage scenarios, and it is discovered that they are largely stable for 30 days and that the storage temperature has no impact on the sensor stability. The performance of the sensors is further assessed using synthetic urine that had been spiked, and the recovery rates found suggest that there is a chance the technology will be used in matrices that are encountered in the real world.

4. Conclusion and future work

In this study, we have developed a scalable, low-cost method for fabricating PVA/r-GO/PEI-based electrodes on ITO-coated glass substrates. The electrodes' biosensing abilities are demonstrated by their capacity to identify E. coli in synthetic urine and PBS. With a LOD of 285 CFU/mL, our proof-of-concept sensing tool could detect *E*. coli in human urine at 915 to 2.5×10^{-7} CFU/mL concentrations. We believe the platform may recognize other germs or symptoms by simply changing the antibodies. Transferring these graphene-based sensors onto different substrates for use in other sensing applications, such as wearable sensing, would be exciting. A preliminary

study suggests that these nanocomposite films may be used on a variety of other substrates. It is so tiny that it could be turned into a microelectrode utilising our technology. Future research will concentrate on enhancing printing and stamping onto other surfaces for various applications as well as leveraging this method to create microelectrode arrays.

Conflict of Interest

There is no conflict of interest.

Supporting Information

Not applicable.

References

[1] A. A. Lahcen, S. Rauf, T. Beduk, C. Durmus, A. Aljedaibi, S. Timur, H. N. Alshareef, A. Amine, O. S. Wolfbeis, K. N. Salama, Electrochemical sensors and biosensors using laser-derived graphene: a comprehensive review, *Biosensors and Bioelectronics*, 2020, **168**, 112565, doi: 10.1016/j.bios.2020.112565.

[2] P. Parthasarathy, Synthesis and UV detection characteristics of TiO_2 thin film prepared through Sol gel route, *IOP Conference Series: Materials Science and Engineering*, 2018, **360**, 012056, doi: 10.1088/1757-899x/360/1/012056.

[3] R. Tortorich, H. Shamkhalichenar, J.-W. Choi, Inkjet-printed and paper-based electrochemical sensors, *Applied Sciences*, 2018, **8**, 288, doi: 10.3390/app8020288.

[4] A. Alavudeen Basha, S. Vivekanandan, P. Parthasarathy, Evolution of blood pressure control identification in lieu of post-surgery diabetic patients: a review, *Health Information Science and Systems*, 2018, **6**, 1-10, doi: 10.1007/s13755-018-0055-z.

[5] J. L. Hammond, N. Formisano, P. Estrela, S. Carrara, J. Tkac, Electrochemical biosensors and nanobiosensors, *Essays in Biochemistry*, 2016, **60**, 69-80, doi: 10.1042/ebc20150008.

[6] S. Vivekanandan, P. Parthasarathy, A comprehensive review on thin film-based nano-biosensor for uric acid determination: arthritis diagnosis, *World Review of Science, Technology and Sustainable Development*, 2018, **14**, 52, doi: 10.1504/wrstsd.2018.10013891.

[7] S. K. Krishnan, E. Singh, P. Singh, M. Meyyappan, H. S. Nalwa, A review on graphene-based nanocomposites for electrochemical and fluorescent biosensors, *RSC Advances*, 2019, **9**, 8778-8881, doi: 10.1039/c8ra09577a.

[8] P. Parthasarathy, S. Vivekanandan, A typical IoT architecture-based regular monitoring of arthritis disease using time wrapping algorithm, *International Journal of Computers and Applications*, 2020, **42**, 222-232, doi: 10.1080/1206212X.2018.1457471.

[9] E. Singh, M. Meyyappan, H. S. Nalwa, Flexible graphene-based wearable gas and chemical sensors, *ACS Applied Materials & Interfaces*, 2017, **9**, 34544-34586, doi: 10.1021/acsami.7b07063.

[10] Y. Z. N. Htwe, M. Mariotti, Printed graphene and hybrid conductive inks for flexible, stretchable, and wearable electronics: progress, opportunities, and challenges, *Journal of Science: Advanced Materials and Devices*, 2022, **7**, 100435, doi: 10.1016/j.jsamd.2022.100435.

[11] P. Parthasarathy, S. Vivekanandan, A numerical modelling of an amperometric-enzymatic based uric acid biosensor for GOUT arthritis diseases, *Informatics in Medicine Unlocked*, 2018, **12**, 143-147, doi: 10.1016/j.imu.2018.03.001.

[12] N. Nagarajan, P. Panchatcharam, Cost-effective and eco-friendly copper recovery from waste printed circuit boards using organic chemical leaching, *Heliyon*, 2023, **9**, e13806, doi: 10.1016/j.heliyon.2023.e13806.

[13] K. S. Novoselov, V. I. Fal'ko, L. Colombo, P. R. Gellert, M. G. Schwab, K. Kim, A roadmap for graphene, *Nature*, 2012, **490**, 192-200, doi: 10.1038/nature11458.

[14] P. Parthasarathy, S. Vivekanandan, A. Basha A, Structural, optical and electrochemical response studies of TiO_2-ZrO_2 nanocomposite for uric acid detection. 2019 Innovations in Power and Advanced Computing Technologies (i-PACT), Vellore, India. IEEE, 2020, 1-6, doi: 10.1109/i-PACT44901.2019.8960032.

[15] H. Zhang, H. Zhang, A. Aldalbahi, X. Zuo, C. Fan, X. Mi, Fluorescent biosensors enabled by graphene and graphene oxide, *Biosensors and Bioelectronics*, 2017, **89**, 96-106, doi: 10.1016/j.bios.2016.07.030.

[16] P. Parthasarathy, S. Vivekanandan, An extensive study on the COVID-19 pandemic, an emerging global crisis: risks, transmission, impacts and mitigation, *Journal of Infection and Public Health*, 2021, **14**, 249-259, doi: 10.1016/j.jiph.2020.12.020.

[17] N. K. Mishra, N. Patil, M. Anas, X. Zhao, B. A. Wilhite, M. J. Green, Highly selective laser-induced graphene (LIG)/polysulfone composite membrane for hydrogen purification, *Applied Materials Today*, 2021, **22**, 100971, doi: 10.1016/j.apmt.2021.100971.

[18] Y. Chyan, R. Ye, Y. Li, S. P. Singh, C. J. Arnusch, J. M. Tour, Laser-induced graphene by multiple lasing: toward electronics on cloth, paper, and food, *ACS Nano*, 2018, **12**, 2176-2183, doi: 10.1021/acsnano.7b08539.

[19] P. Parthasarathy, S. Vivekanandan, Urate crystal deposition, prevention and various diagnosis techniques of GOUT arthritis disease: a comprehensive review, *Health Information Science and Systems*, 2018, **6**, 1-13, doi: 10.1007/s13755-018-0058-9.

[20] Y. Jung, J. Min, J. Choi, J. Bang, S. Jeong, K. R. Pyun, J. Ahn, Y. Cho, S. Hong, S. Hong, J. Lee, S. H. Ko, Smart paper electronics by laser-induced graphene for biodegradable real-time food spoilage monitoring, *Applied Materials Today*, 2022, **29**, 101589, doi: 10.1016/j.apmt.2022.101589.

[21] P. Parthasarathy, S. Vivekanandan, Biocompatible TiO_2-CeO_2 Nano-composite synthesis, characterization and analysis on electrochemical performance for uric acid determination, *Ain Shams Engineering Journal*, 2020, **11**, 777-785, doi: 10.1016/j.asej.2019.11.011.

[22] M. F. El-Kady, V. Strong, S. Dubin, R. B. Kaner, Laser scribing of high-performance and flexible graphene-based electrochemical capacitors, *Science*, 2012, **335**, 1326-1330, doi: 10.1126/science.1216744.

[23] P. Parthasarathy, S. Vivekanandan, Investigation on uric acid biosensor model for enzyme layer thickness for the application of arthritis disease diagnosis, *Health Information Science and Systems*, 2018, **6**, 1-6, doi: 10.1007/s13755-018-0043-3.
[24] V. Strong, S. Dubin, M. F. El-Kady, A. Lech, Y. Wang, B. H. Weiller, R. B. Kaner, Patterning and electronic tuning of laser scribed graphene for flexible all-carbon devices, *ACS Nano*, 2012, **6**, 1395-1403, doi: 10.1021/nn204200w.
[25] B. van Grinsven, K. Eersels, O. Akkermans, S. Ellermann, A. Kordek, M. Peeters, O. Deschaume, C. Bartic, H. Diliën, E. Steen Redeker, P. Wagner, T. J. Cleij, Label-free detection of Escherichia coli based on thermal transport through surface imprinted polymers, *ACS Sensors*, 2016, **1**, 1140-1147, doi: 10.1021/acssensors.6b00435.